J Solid State Electrochem (2008) 12:225–236
DOI 10.1007/s10008-007-0381-6

ORIGINAL PAPER

Effect of H_2SeO_3 on the early stages of nucleation and growth during Cu electrocrystallization in acidic medium on glassy carbon electrode

Dijana Šimkūnaitė · Emilija Ivaškevič · Ignas Valsiūnas · Aleksandras Kaliničenko · Antanas Steponavičius

Received: 2 February 2007 / Revised: 18 April 2007 / Accepted: 14 June 2007 / Published online: 19 July 2007

Abstract The early stages of Cu electrodeposition onto a GC electrode were investigated in 0.5 M H_2SO_4+0.01 M $CuSO_4$ solution without or with H_2SeO_3 when a molar concentration ratio [Cu(II)]/[Se(IV)] was 1.10^4 to 2.10^2. The H_2SeO_3 solution in 0.5 M H_2SO_4 was also used. The electrochemical techniques such as cyclic voltammetry and chronoamperometry and structural investigation using ex situ AFM were applied to study the nucleation and growth of Cu onto a GC electrode. Chronoamperometric results were shown to follow an instantaneous 3D nucleation and diffusion-controlled growth model by Scharifker and Hills. The values of number of Cu nuclei N and average nuclei radius r_{av} were calculated. It was shown that, in the presence of H_2SeO_3 in amounts of 0.001 to 0.005 mM, N increases and r_{av} decreases. At higher concentrations of the additive, the changes of these parameters with the deposition potential E_{dep} were shown to be somewhat more complex. The dependences of N and r_{av} on the concentration of H_2SeO_3 in different regions of Cu overpotentials were also revealed.

Keywords Copper · Electrodeposition · Early stages · Selenious acid · Glassy carbon electrode · Sulphate solution

D. Šimkūnaitė (✉) · E. Ivaškevič · I. Valsiūnas · A. Kaliničenko · A. Steponavičius
Institute of Chemistry,
Goštauto 9,
01108 Vilnius, Lithuania
e-mail: nemezius@ktl.mii.lt

Introduction

It is well known that the nucleation and growth are very important stages in a metal electrodeposition process [1]. They are usually investigated using foreign substrates, such as platinum, gold and carbon including glassy carbon (GC). Particularly important studies have been performed applying a GC electrode. Among the specific properties of this electrode are good electrical conductivity and high surface quality with excellent polishing characteristics.

Copper is known to be one of the most commonly used functional metals because of its industrial importance and great suitability for studying the kinetics and mechanism of the metal electrocrystallization process onto foreign substrates [1–3]. The electrodeposition of Cu onto a GC electrode from acidic solutions is well documented [4–11].

Studying the nucleation mechanism of Cu during electrodeposition of thin films from sulphate solutions as a function of solution pH, Cu^{2+} concentration, deposition potential (E_{dep}) and temperature, it has been found that the Cu nuclei size increased and the nuclei number (N) decreased with the increase in pH and Cu^{2+} concentration [5]. The negative shift of E_{dep} produced smaller nuclei and higher Cu nuclei population density. By fitting experimental chronoamperometric data into the Scharifker–Hills nucleation model [9–11], a pH-dependent Cu nucleation mechanism has been found to be reasonable [5]. In particular, it has been established that, at pH 1, in the absence of Na_2SO_4 as a background electrolyte, Cu nucleation is instantaneous, while in the presence of this salt the mechanism is mixed.

No Cu adlayers formation onto a stationary or rotating GC ring-disk electrode has been found during potentiodynamic Cu deposition from sulphate solutions of pH 0.3 at

potentials (*E*s) more positive than an equilibrium potential (E_{eq}) of a reversible Cu electrode [6]. It has been supposed that the oxygen-containing surface groups of a GC electrode can be active centres for the discharge of Cu^{2+} ions and the nucleation of new phase. On the basis of the chronoamperometric data, the charge transfer kinetics has been stated to be the determining factor—the discharge of Cu^{2+} ions is accelerated in the presence of specifically adsorbed anions and own oxygen-containing surface groups of GC [7]. One of the reasons for the accelerated Cu deposition onto GC has been supposed to be a parallel-to-the surface flow of univalent Cu ions that can be formed on vacant parts of the GC electrode. It has again been stated that the oxygen-containing surface groups of GC are, probably, active centres for the processes of discharge of Cu^{2+} ions and nucleation of the new phase [7].

When studying the nucleation and growth of Cu on a GC electrode under potentiostatic conditions, the current transients at short times and relatively low overpotentials have been interpreted in terms of progressive nucleation and growth with bearing in mind the combined charge transfer and diffusion limitations of the growth of supercritical Cu crystals [9, 10]. The influence of ion transfer and electron transfer electron reactions taking place before and simultaneously with the process of Cu nucleus formation have also been discussed [9, 10]. The nucleation and growth of Cu crystals on a GC electrode in an extended overpotential interval has been investigated in [11]. A good qualitative agreement has been found between the experimental data relating the current transients [11] and the models developed for progressive nucleation on a limited number of active sites and for instantaneous nucleation [12–16].

It is commonly known that the microstructure and morphology of electrodeposited thin metal films can be controlled by the addition of additives to plating solutions. Concerning the application of additives for the Cu electrodeposition and, particularly, for the kinetics of early stages of Cu nucleation and growth, it has recently been shown that some promising advantages can be obtained with a polycrystalline Pt electrode when H_2SeO_3 is present in a solution [17, 18]. While the codeposition of Cu and Se onto various substrates and the formation of thin layers of copper selenides have already been investigated extensively (for example, see [18]), both the discharge and the crystallization of Cu onto a foreign substrate have been studied to a lesser extent. It has been shown that much less amounts of Se(IV) compounds namely, ranging from 10^{-6} to 10^{-4} M, and at a molar concentration ratio [Cu(II)]/[Se(IV)] from 10^2 to 10^5 are typically used when the discharge reaction of Cu^{2+} ions itself is to be studied, as compared with the electrodeposition of copper selenides, when the comparable amounts of Cu(II) and Se(IV) are commonly applied [19–24]. Moreover, the acceleration of Cu^{2+} discharge in acidic Cu^{2+} solutions possible due to so-called catalytic ox/red cycle (CORC) has also been studied in the presence of small amounts of Se(IV) [25–27].

While various aspects of the Cu electrodeposition in the presence of H_2SeO_3, as mentioned above, have been described earlier, there have been no reports about the early stages of Cu electrocrystallization onto a GC electrode in the presence of small amounts of H_2SeO_3.

The present work deals with the examination of the effect of H_2SeO_3 on the early stages of Cu nucleation and growth onto a GC electrode in an acidic $CuSO_4$ solution. Some attention was also given to the electrochemical behaviour of H_2SeO_3 onto a GC electrode in the absence of Cu^{2+} ions. As a matter of fact, this paper does not deal with the formation of copper selenides as a semiconducting material.

Experimental

The working solution was 0.5 M H_2SO_4+0.01 M $CuSO_4$ containing H_2SeO_3 in amounts of 1.10^{-3} to 5.10^{-2} mM. In separate experiments, the solution 0.5 M H_2SO_4 +H_2SeO_3 in amounts of 0.01 or 0.1 mM was also used. In the Cu^{2+}-containing solutions, the molar concentration ratio [Cu(II)]/[Se(IV)] was no less than 2.10^2. The working solution was prepared from triply distilled water, copper sulphate (Fluka) preheated at 400 °C for 4 h, highest purity sulphuric acid (Russia) and selenious acid (99.999% purity, Aldrich). Before each experiment, the working solution was de-aerated with Ar gas for 0.5 h.

All electrochemical experiments were carried out at 20± 0.1 °C in a conventional three-electrode cell. The working electrode was a vertical disc with a diameter of 0.5 cm made from glassy carbon rod (Sigradur G). The electrode was cemented into a glass tube. The counter electrode was a Pt sheet of ca. 4 cm^2 in area, and the reference electrode was a Cu wire additionally coated with electrolytic Cu and immersed in the working solution. In the text, all potentials (*E*s) were recalculated with respect to the standard hydrogen electrode, unless otherwise stated.

The pretreatment of the GC electrode prior each electrochemical measurement was as follows: (1) mechanical polishing to a nearly mirror finish with successively finer grades of alumina powders, eventually to 0.05 μm, and cleaned ultrasonically in sequence in acetone, diluted HCl and triply distilled water; (2) to obtain a clean reproducible surface before each following measurement, the GC electrode was also scanned in the background 0.5 M H_2SO_4 solution at a potential scan rate 50 mV s^{-1} for 0.5 h between E_{sc}≈+0.25 and E_{sa}≈+0.8 V.

The electrochemical investigations were carried out using the cyclic voltammetry and single potential step

techniques. The value of E_{start} was +0.8 V. The cyclic voltammograms (CVs) and potentiostatic *I*/*t* curves were recorded using a PI 50-1 potentiostat (Belarus) interfaced through a homemade analogue to digital converter with a PC (Siemens) and a PR-8 programmer (Belarus).

The samples for the ex situ AFM investigations were prepared by imposing a potentiostatic pulse to a given deposition time (t_{dep}). The AFM observation was performed using a TopoMetrix Explorer SPM with a Si_3N_4 tip operating in a contact mode. The top view images are presented in so-called "height mode" where the higher parts appear brighter. A cross-sectional analysis of an AFM image was also applied.

The Nernst potential (E_{eq}) for a couple Cu^{2+}/Cu was estimated by measuring an open-circuit potential of bulk Cu in unstirred 0.5 M H_2SO_4+0.01 M $CuSO_4$ solution at 20 °C and was found to be equal to +0.260 V.

Results and discussion

System GC/H_2SO_4 + H_2SeO_3

Considerable work has already been done on the electrochemical reduction of selenious acid onto different substrates (e.g., see a review work [28]). Most attention has been paid to the reduction of Se(IV) onto Pt and Au electrodes. Only some reports, e.g. [29], deal with electrochemistry of Se(IV) onto a GC electrode.

The following sequence has been proposed for the reduction of H_2SeO_3 onto such noble metals as Au and Pt and also onto carbon electrodes [30]:

$$H_2SeO_3 + 6H^+ + 6e \rightarrow H_2Se + 3H_2O, \quad (1)$$

followed by the chemical reaction

$$2H_2Se + H_2SeO_3 \rightarrow 3Se + 3H_2O. \quad (2)$$

The rate of the chemical reaction (2) has been shown to be dependent on the concentration of H_2SeO_3, therefore at higher concentrations of this reactant the reaction (2) is fast, and the overall process taking place at the electrode surface appears to be four-electron reaction:

$$H_2SeO_3 + 4H^+ + 4e \rightarrow Se + 3H_2O. \quad (3)$$

Studying the electrochemical behaviour of H_2SeO_3 onto GC electrodes in different acidic media, including 0.5 M H_2SO_4 solution, by cyclic and stripping voltammetry, only poorly defined voltammetric curves with a single cathodic peak c3 at E_{pc3} about −0.80 V vs SCE have been recorded [29]. It has also been found that anodization of an electrode at *E*, where oxygen evolves, leads to a slight shift of a whole voltammetric curve upward, but a general shape of the curve remains unchanged. In general, the results presented in [29, 30] have indicated that the behaviour of H_2SeO_3 depends markedly on the kind and pretreatment modes of carbon electrodes used.

Taking into account the circumstances mentioned above, the conduction of several introductory experiments with the GC electrode applied in our work might be thought as being quite justified.

Figure 1 shows the CVs recorded for the GC electrode in 0.5 M H_2SO_4 solution where H_2SeO_3 is the only electroactive species within the anodic limit E_{sa}=+0.80 V and cathodic limit E_{sc}=−0.20 V. In the case of the solution with higher concentration of reactant, a single cathodic peak at E_{pc} about −0.14 V was revealed (Fig. 1b). In the less concentrated solution, the shoulder-like wave appeared (Fig. 1a). In both cases, it was obtained that with each successive full cycle the height of the shoulder-like wave (Fig. 1a) or the peak (Fig. 1b) decreases, maybe, as proposed in [30], due to the formation of a passivating surface selenium film.

As shown in Fig. 2a, no defined cathodic current peaks were obtained for the GC electrode at *E* more positive than E_{pc} in Fig. 1, even when the CVs were recorded after anodic going sweeps to high positive *E*. If the cathodic limit E_{sc} was shifted slightly negative to E_{pc} in Fig. 1, e.g. to −0.3 V (E_{sc2} in Fig. 2b), the general shape of voltammetric response remained unchanged. With the further negative shift of E_{sc}, up to *E* of hydrogen evolution,

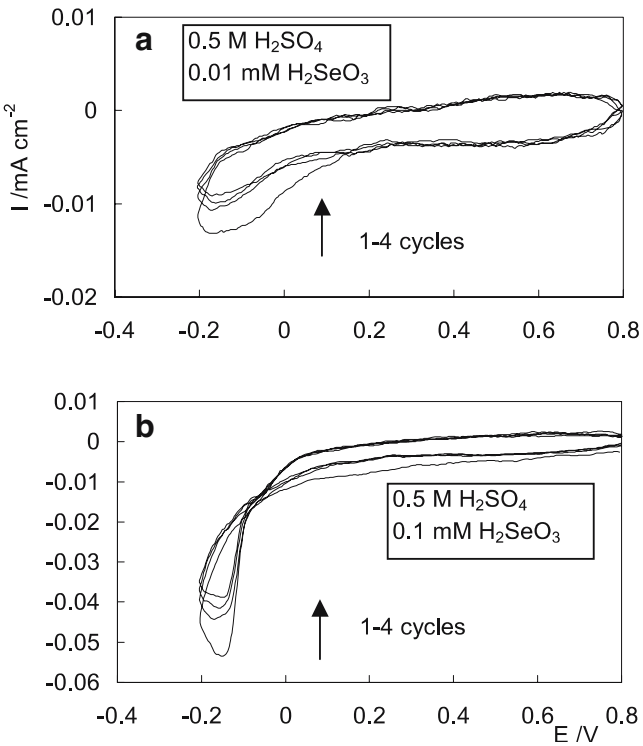

Fig. 1 Typical cyclic voltammograms for GC electrode in 0.5 M H_2SO_4 solution containing 0.01 (**a**) or 0.1 (**b**) mM H_2SeO_3 at a scan rate v=10 mV s^{-1} between $E_{s,a}$=+0.80 V and $E_{s,c}$=−0.20 V

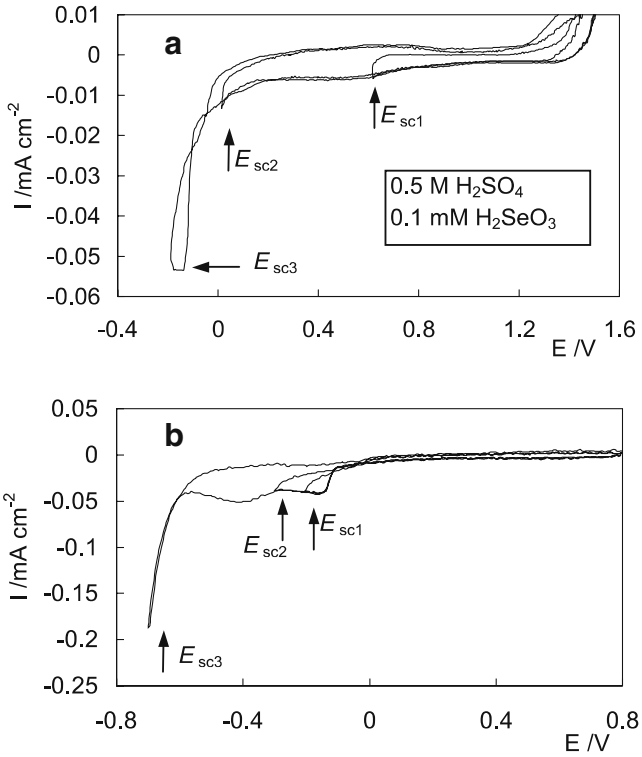

Fig. 2 Typical cyclic voltammograms (the 3rd cycles) for GC electrode in 0.5 M H_2SO_4+0.1 mM H_2SeO_3 solution at a scan rate v=10 mV s^{-1} between $E_{s,a}$=+1.5 V and $E_{s,c}$=−0.20 V (**a**) and between $E_{s,a}$=+0.8 V and different values of $E_{s,c}$ (**b**)

the additional rather well defined broad cathodic peak can be revealed at about −0.4 V (Fig. 2b). At the moment, the nature of this peak is not clear. It is interesting, however, to note that the appearance of two cathodic peaks, the first well developed probably adsorptive peak at less negative E, followed by an ill developed one at more negative E, has been observed when a carbon paste electrode with dispersed selenite was used for the experiments [31]. The authors have attributed these individual peaks to the consecutive electron transfers, involving the formation of Se(0) as an intermediate.

Systems GC/H_2SO_4 + $CuSO_4$ and GC/H_2SO_4 +$CuSO_4$ + H_2SeO_3

Figure 3a shows the voltammetric response for the negative (forward) and positive (reversal) going sweeps for the GC electrode in the solution 0.5 M H_2SO_4+0.01 M $CuSO_4$ in the potential region in which Cu underpotential deposition is usually observed onto a foreign metal substrate. In accordance with the earlier results [6], no Cu adlayers onto GC were found in this E region. When H_2SeO_3 was added to the solution, a single cathodic current peak at about +0.30 V appears. This peak increases with the increase in the concentration of additive and in the number of successive full cycles (Fig. 3b–d). A slight dependence of E_{pc} on the same factors was also observed−E_{pc} slightly shifted in the negative direction. Upon the reversal sweeps, a small anodic current peak begins to be visible. Such an

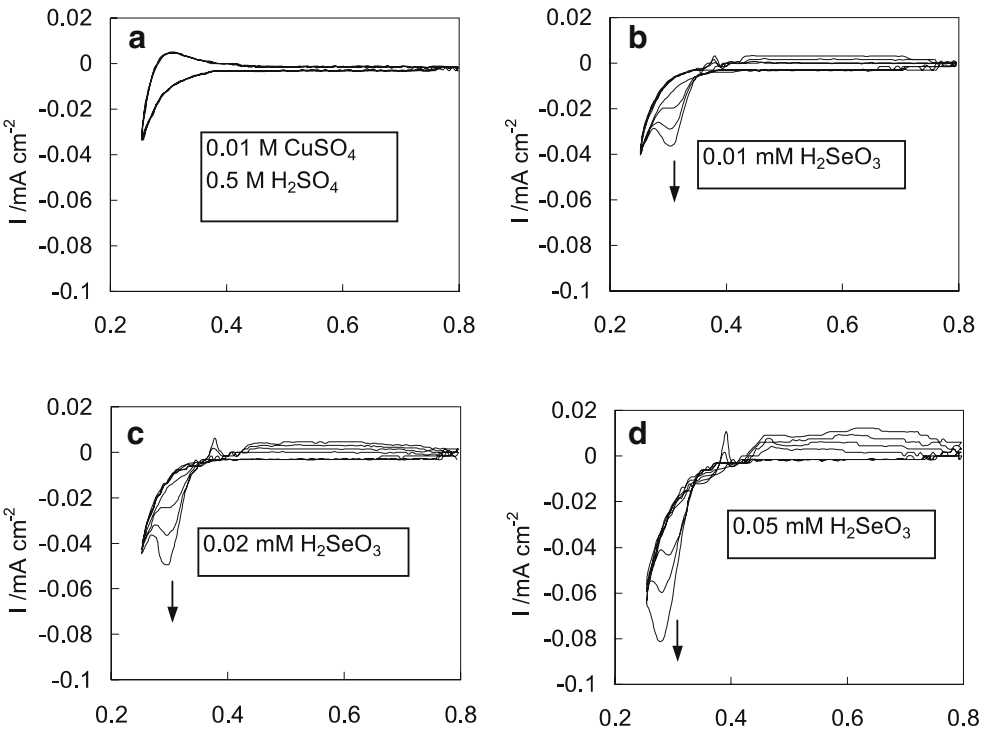

Fig. 3 Typical cyclic voltammograms for GC electrode in 0.5 M H_2SO_4+0.01 M $CuSO_4$ solution **(a)** containing increasing amounts of H_2SeO_3 **(b-d)**. Successive cycling at v=10 mV s^{-1} between $E_{s,a}$=+0.8 V and $E_{s,c}$=+0.25 V (E_{sc}>E_{eq})

anodic peak was not observed for the separate systems H_2SO_4+H_2SeO_3 and H_2SO_4+$CuSO_4$. As can be seen from the anodic portions of CVs, there is a tendency for the height of this peak to increase with the bulk concentration of H_2SeO_3.

Although the experimental conditions applied in our study and those in [19] differ quite significantly, especially as to the values of ratio of molar concentrations [Cu(II)]/[Se (IV)], in particular, 10^3 to 2.10^2 vs 0.1, respectively, it seems possible to compare formally these two instances. Then, the development of the cathodic current peaks (Fig. 3b–d) in the presence of H_2SeO_3 may be assigned to the formation of non-stoichiometric compound $Cu_{2-x}Se$ according to the equation [14]:

$$H_2SeO_3 + (2 - x)Cu^{2+} + 4H^+ + (7 - x)e \rightarrow Cu_{2-x}Se + 3H_2O \quad (4)$$

From the analysis of the ratio of the limiting currents corresponding to copper selenide formation and that corresponding to the reaction $Cu^{2+} + 2e \rightarrow Cu^0$, it has been concluded that some of the sites in the compound CuSe can exist in the Cu(I) state [19]. It has also been assumed that the latter factor can be considered as one of possible reasons causing the formation of non-stoichiometric $Cu_{2-x}Se$ rather than the stoichiometric CuSe.

When the potential sweeps were extended into a region characteristic of the overpotential deposition of Cu layer, in particular, to $E_{s,c}$=−0.20 V, the set of CVs was recorded depending on the concentration of H_2SeO_3 and the number of successive full cycles. Figure 4a shows the representative current-potential profile for the GC electrode in the pure 0.5 M H_2SO_4+0.01 M $CuSO_4$ solution at a sweep rate (v) 10 mV s^{-1} between the anodic limit +0.80 V and the cathodic limit −0.20 V. As is seen, on the return scan, a typical nucleation loop was obtained, involving a cathodic current greater than recorded in the preceding negative potential scan. It should be noted, that the voltammetric responses for the GC electrode in the acidic $CuSO_4$ solution used here are similar to those described earlier for the electrodeposition of Cu onto a GC electrode or onto other foreign substrates (e.g., see [3, 5, 6, 9, 17, 32]). Therefore, there is no need to go into the details of the CVs presented here.

Both the addition of H_2SeO_3 and the application of the consecutive sweeps resulted in a change of this profile (Figs. 4b,c and 5). Firstly, the voltammetric curves recorded onto the GC in the presence of H_2SeO_3 are characterized by two waves. The first current peak with E_p in the region of +0.30 V (Fig. 4b,c), i.e. in fact in the same E region as in the case of cathodic going scans in more narrow E window (Fig. 3). This peak is followed by the second current peak that is attributed to the electrodeposition of Cu layer. The

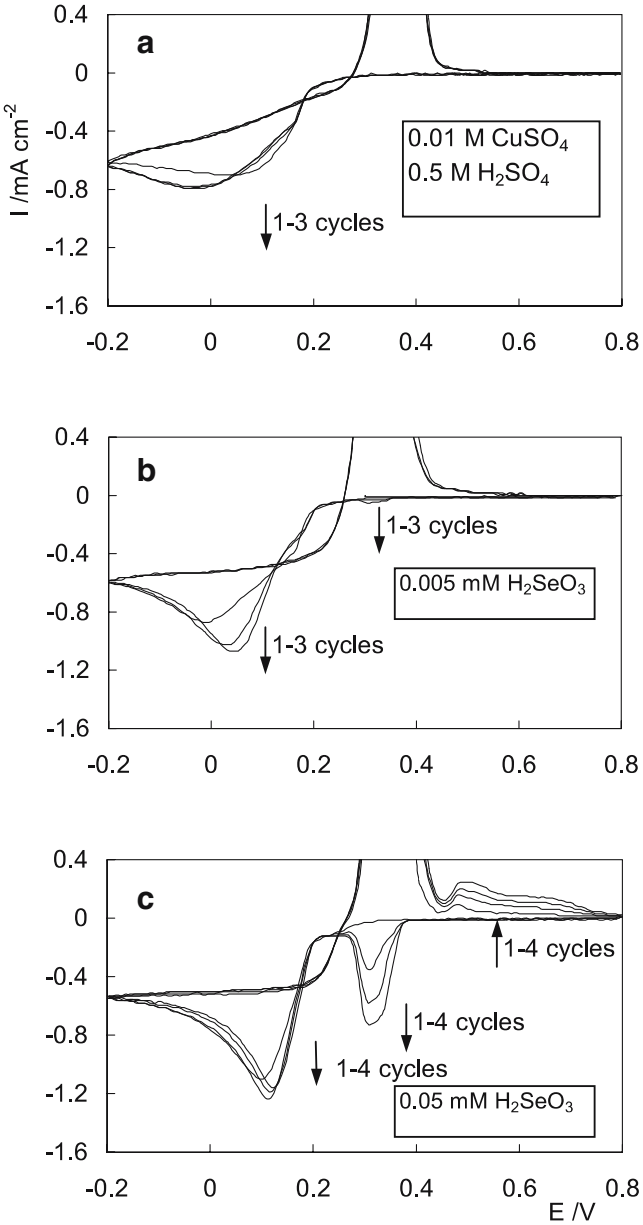

Fig. 4 Successive cyclic voltammograms for GC electrode in 0.5 M H_2SO_4+0.01 M $CuSO_4$ solution without (**a**) or with 0.005 (**b**) or 0.05 (**c**) mM H_2SeO_3 at v=10 mV s^{-1} between $E_{s,a}$=+0.80 V and $E_{s,c}$= −0.20 V (E_{sc}<E_{eq})

height and the peak potential E_{pc} of this peak were found to be Se(IV)-dependent namely, I_{pc} increases and E_{pc} somewhat becomes more positive with increasing the bulk concentration of H_2SeO_3 (Fig. 4b,c). Secondly, it should be specifically pointed out that whereas the first wave was not, under any circumstances, observed in the pure acidic $CuSO_4$ solution, it became visible beginning with even the smallest concentration of H_2SeO_3 used in our study (Fig. 4). Thirdly, if the whole interval of concentrations of H_2SeO_3, from 0.005 to 0.1 mM, is taken into account, there is no clear proportionality between the increase in the height of the first current peak with increasing the amount

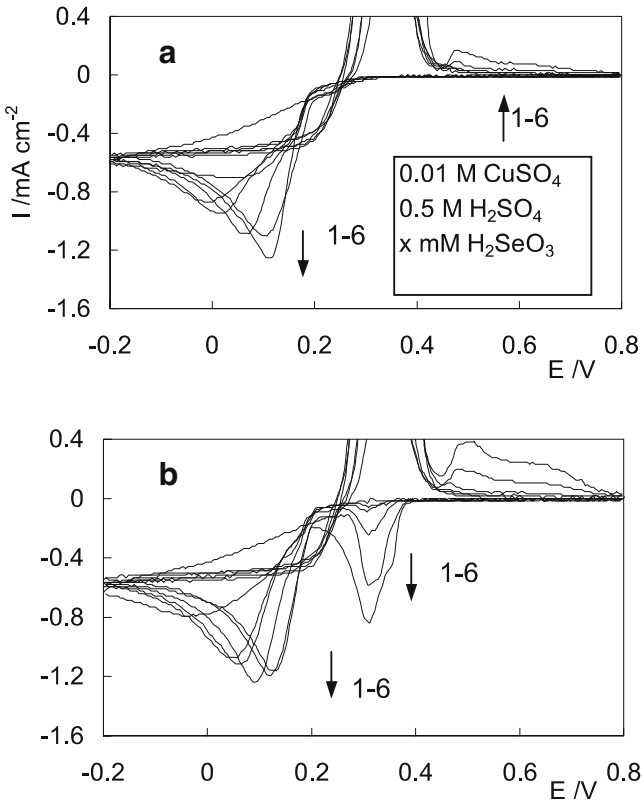

Fig. 5 Successive cyclic voltammograms for GC electrode in 0.5 M H_2SO_4+0.01 M $CuSO_4$ solution containing increasing amounts of H_2SeO_3 at v=10 mV s^{-1} between $E_{s,a}$ and $E_{s,c}$ as in Fig. 4. Concentration of H_2SeO_3: 1-0, 2-0.005, 3-0.01, 4-0.02, 5-0.05, 6-0.1 mM. The first cycles (**a**) and the third cycles (**b**)

of the additive and the extent to which the height of the second peak I_{pc} is affected by the presence of H_2SeO_3 (Fig. 5b). Finally, it is the authors' opinion that the following strongly pronounced feature of the recorded CVs should be also stressed. Whereas the development of the first current peak was not observed at all during the initial (first) cathodic scan (Fig. 5a), this peak was found to appear and his height to increase as the number of sweeps was further increased, when at least four full consecutive sweeps were made (Fig. 4c). Such peculiarities of the CVs, especially the dependencies of the shape of these curves in the region of the first current peak on the concentration of H_2SeO_3 and on the consecutive cycling, may be indicative for the formation of a solid surface compound. Then, the initially bare surface of the GC electrode may be considered as being somewhat modified, and, if this is the case, the effect of such a modification on the electrocrystallization of Cu may also be expected.

Chronoamperometric experiments were further performed to investigate in more detailed way the nucleation and growth mechanism for the Cu particles. By applying a set of potential steps that started at E_{start}=+0.80 V to E_{dep} between +0.10 and −0.10 V, a family of current-time (I/t) curves for Cu electrodeposition onto the GC electrode for various applied potentials was recorded (Fig. 6). After sharp decrease in the current at very short time related to the double layer charging and also to the occurrence of the electrochemical reaction Cu^{2+}→Cu as proposed in [9], the ascending part of the transients are observed. The current

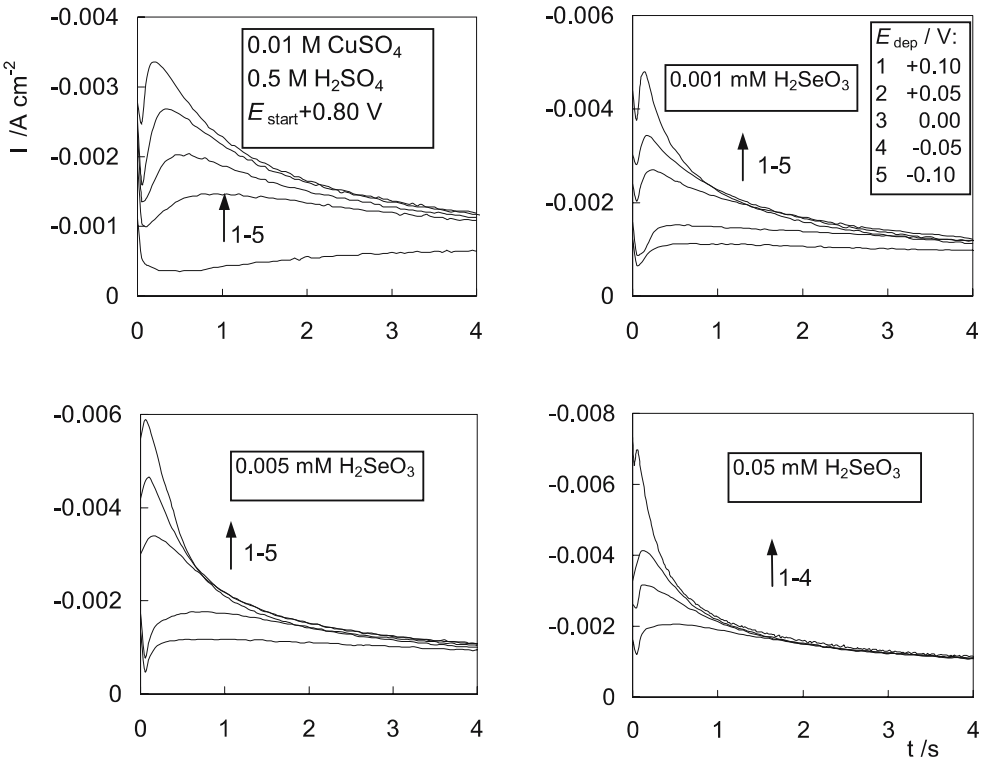

Fig. 6 Potentiostatic current transients for the Cu electrodeposition onto GC electrode recorded by E steps from E_{start}= +0.80 V to different deposition potentials E_{dep} (E_{dep}<E_{eq}) in 0.5 M H_2SO_4+0.01 M $CuSO_4$ solution containing different amounts of H_2SeO_3

increases with time and passes through a maximum value (I_{max}) at the time t_{max}. In fact, these transients are typical of those for the 3D nucleation and growth of a new phase at a foreign substrate surface [1]. As the E_{dep} is moved progressively towards lower values, there is the increase in I_{max} and the decrease in t_{max} (Fig. 6). The addition of H_2SeO_3 to the working solution was found to result in the increase in I_{max} and, correspondingly, in the decrease in t_{max}.

According to the theory of Scharifker and Hills (SH model) [14], the rise in current corresponds to the increase in the electroactive area. This increase in area, limited by spherical diffusion around each nucleus, is accepted to be due to the increase in the nucleus size and/or the increase in the number of nuclei (N). In multiple nucleations, two limiting cases have to be considered depending on high or low nucleation rate is characteristic for a system. At high nucleation rate, all the nuclei are immediately created and their number remains constant during the growth process, i.e. instantaneous nucleation occurs. At low nucleation rate, new nuclei are continuously formed during the whole deposition process, i.e. progressive nucleation occurs. One of methods for distinguishing between these two limiting cases is to compare the experimental transients plotted in a non-dimensional plot, $(I/I_{max})^2$ vs t/t_{max}, with the corresponding plots for the instantaneous and progressive 3D nucleation and growth. According to the SH model [14], for the instantaneous 3D nucleation with diffusion-controlled growth process:

$$(I/I_{max})^2 = 1.9542(t/t_{max})^{-1}\{1 - \exp[-1.2564(t/t_{max})]\}^2, \quad (5)$$

and for the progressive 3D nucleation with diffusion-controlled growth process:

$$(I/I_{max})^2 = 1.2254(t/t_{max})^{-1}\left\{1 - \exp\left[-2.3367(t/t_{max})^2\right]\right\}^2. \quad (6)$$

It is well known that, at present, there is considerable debate about the application of the SH model [14] or the more general model, by Scharifker and Mostany (SM) which allows the consideration of two extreme cases of nucleation to be eliminated, in comparison to other models proposed by other authors, e.g. Heerman and Tarallo, Sluyters-Rehbach, Mirkin and Nilov, etc. Nevertheless, the SH model seems to be most commonly used to describe the early stages of metal electrocrystallization in different real systems [33]. Because of this, the SH model was also applied in our work.

The experimental $(I/I_{max})^{2+}$ vs t/t_{max} plots along with the plots calculated from Eqs. 5 and 6 are shown in Fig. 7. The experimental curves fitting in terms of the SH model reveals that within the whole E_{dep} region applied a rather good correlation with the theoretical curve for instantaneous nucleation is obtained both for the pure $CuSO_4$ solution (Fig. 7a) and that containing H_2SeO_3 (Fig. 7b–d),

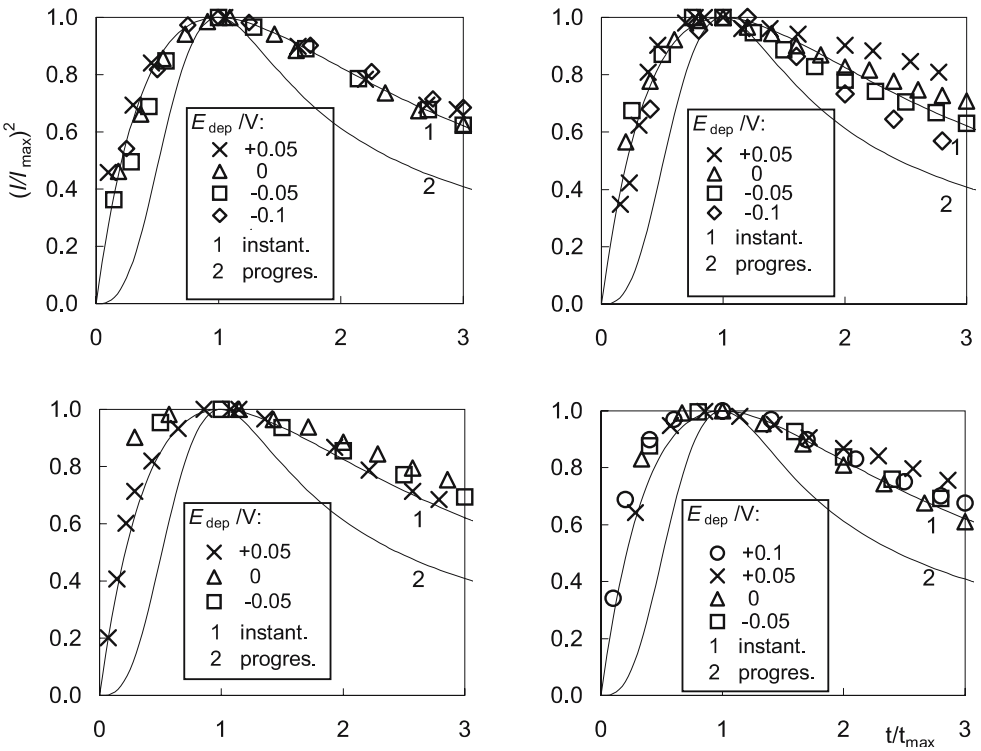

Fig. 7 Nondimensional plots of the potentiostatic current transients recorded onto GC electrode in 0.5 M H_2SO_4+ 0.01 M $CuSO_4$ solution containing different amounts of H_2SeO_3 (data from Fig. 6). *Lines*, theoretical instantaneous (*1*) and progressive (*2*) 3D nucleation and diffusion-controlled growth according to the SH model

i.e. the Cu nucleation mode remains unchanged with adding H_2SeO_3, similarly as in the case of the system Pt/H_2SO_4+$CuSO_4$+H_2SeO_3 [18].

Once it is established that the instantaneous 3D nucleation with diffusion-controlled growth SH model is applicable for the Cu deposition onto the GC electrode, the number density of formed Cu nuclei at different E_{dep} can be calculated from the values of I_{max} and t_{max} in the chronoamperograms [14], using a more convenient relationship [5]:

$$N = 0.065(zFc/I_{max}t_{max})^2 \Big/ k_e, \quad (7)$$

where zF is the molar charge transferred during electrodeposition, c is the concentration of metal ions, the material constant $k_e=(8\pi cM/\rho)^{0.5}$, M and ρ are the molar weight and density of deposited metal. A parameter k_e for Cu is equal to 0.042.

Recently, Milchev and Heerman [34] have proposed a different way of interpreting the current transients. They have transformed the equations derived earlier by Scharifker and Mostany [15], Mirkin and Nilov [35] and Heerman and Tarallo [16] accounting for the possible limited number of active sites onto a substrate surface and also avoiding underestimation of the current at short times or overestimation of the current in the long time. The experimental data obtained during the electrodeposition of Ag on a GC electrode have been analysed, and the information has been obtained on the applicability of the new theoretical equation for the estimation of $N(t)$ and $I(t)$ of progressive nucleation at the time region before I_{max} [34]. For the case of instantaneous nucleation the new formula [34] has been suggested to be in the form [36]:

$$\ln\ln\left(1-aIt^{1/2}\right)^{-1} = \ln\left(N_o\pi kD\right) + \ln t \quad (8)$$

where $a= \pi^{1/2}/zFD^{1/2}c$ (according the SM model), N_o is the density of active sites and k is the material constant which have been taken to be equal to N and k_e, respectively, D= 5.6.10^{-6} cm^2 s^{-1} [37]. The linear plots of $\ln\ln(1-aIt^{1/2})^{-1}$ vs ln$t$ are shown in Fig. 8. The slope of the straight line for the pure acidic $CuSO_4$ solution is 0.99, which means a good agreement with the theory [34] and also with the earlier work [36] in which the formula (8) has been applied for Rh electrodeposition on a pyrolitic graphite electrode. The calculated value of N was found to be 2.29 ·10^6 cm^{-2}. For the solution containing additive H_2SeO_3 the application of Eq. 8 also resulted in the straight line, its slope, however, is smaller than the expected one by approximately 20% (Fig. 8). Therefore, the type of nucleation for H_2SO_4+$CuSO_4$ solution containing additive H_2SeO_3 was unclassifiable using Eq. 8. In addition, it should be noted that the effect of the concentration H_2SeO_3 on the calculated value of this slope was not clearly defined. The disagreement between the

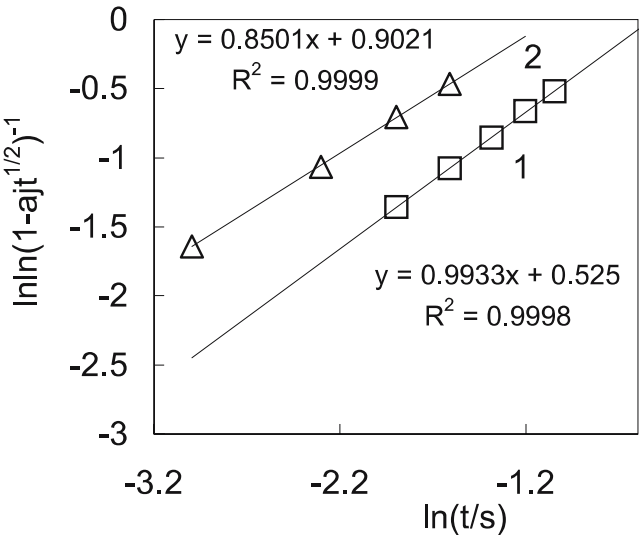

Fig. 8 Data for the current plotted in double logarithmic coordinates according to Eq. 8 for acidic $CuSO_4$ solution without H_2SeO_3 at t less than t/t_{max}=0.64 (*1*) or with 0.001 mM H_2SeO_3 at t less than t/t_{max}= 0.8 (*2*) at E_{dep}=0.0 V

results of the analysis of the chronoamperometric data applying Eqs. 5 and 8 in the presence of H_2SeO_3 is rather unexpected and, at the moment, we have no more reliable explanation for this phenomenon.

The size of individual particle depends on the deposition time (t_{dep}). Once N is estimated from the Eq. 7 and assuming the Cu particles being of hemispherical shape, an average nucleus radius (r_{av}) can be estimated from a charge per unit area of the electrode (Q) consumed during deposition using the properly corrected relation from [38]:

$$r_{av} = (3Qv_m/2\pi zFN)^{1/3}, \quad (9)$$

where v_m is the molar volume of deposited metal, for Cu v_m= 7.1 cm^3 mol^{-1}. Q was evaluated by integrating the corresponding I/t transient over the time interval up to t_{dep}= t_{max} assuming that this quantity of charge is mainly due to a faradaic reaction $Cu^{2+}\rightarrow Cu^0$.

The values of N and r_{av} calculated from the current transients are given in Table 1. The data in Table 1 show that the effect of H_2SeO_3 upon the numerical values of N and r_{av} rather significantly depends first on the region of Cu overpotentials. In particular, in the region of higher overpotentials, say, at E_{dep}=−0.05 V, the addition of H_2SeO_3 causes N to increase clearly with increasing the concentration of additive. At the same time, in the region of lower Cu overpotentials, e.g. at E_{dep}=+0.10 V, the relationship between N and the concentration of H_2SeO_3 is rather poorly apparent. An analogous picture can also be observed for the Se(IV)-dependence of r_{av}.

The morphology of Cu deposited onto the GC electrode was further examined by ex situ AFM (Figs. 9, and 10). In

Table 1 Numerical values of kinetic parameters of the Cu nucleation and growth—nuclei density N and average nucleus radius r_{av}-obtained from analysis of current transients[a] according to the SH [14, 36] and MH [34] models of the Cu electrodeposition onto GC electrode from 0.5 M H_2SO_4+0.01 M $CuSO_4$ solution without or with H_2SeO_3. E_{start}= +0.80 V

H_2SeO_3, mM	E_{dep}, V	$10^3 I_{max}$, (A cm^{-2})	t_{max}, s	$N10^{-6}$ (cm^{-2})		r_{av} (μm)
				From Eq. (7)	From Eq. (8)	
0	0.1	0.66	5.15	0.5		0.49
	0.05	1.46	0.95	2.98		0.20
	0	2.05	055	4.56	2.29	0.16
	−0.05	2.69	0.35	6.52		0.14
	−0.1	3.36	0.20	12.79		0.11
0.001	0.05	1.53	0.8	3.87		0.18
	0	2.70	0.25	12.64		0.10
	−0.05	3.42	0.2	12.34		0.10
	−0.1	4.79	0.13	16.07		0.09
0.005	0.05	1.77	0.7	3.75		0.18
	0	3.39	0.15	22.33		0.07
	−0.05	4.65	0.1	26.62		0.07
	−0.1	5.88	0.05	66.69		0.04
0.05	0.1	2.06	0.5	5.43		0.15
	0.05	3.16	0.18	1.85		0.08
	0	4.12	0.15	15.09		0.09
	−0.05	6.97	0.05	47.47		0.05

[a] Poorly defined transients were not applied for the calculations of nucleation parameters.

all cases, Cu was deposited by a single potential step from E_{start}=+0.80 V to E_{dep}=0.00 V. The electrolysis was terminated after t_{dep}=5, 10 or 30 s. The charges Q calculated from the corresponding transients at t_{dep}=5 s (the AFM images presented below are related to this length of electrolysis) were found to be ca. 7.3 mC cm^{-2} in the absence of H_2SeO_3 and ca. 8.3 mC cm^{-2} in the presence of 0.005 mM H_2SeO_3. Then, it can be suggested that the amount of deposited Cu corresponds to ca. 16.2 or 18.5 equivalent monolayers, respectively.

After the electrodeposition of Cu from the pure working electrolyte for 5 s, it was found that the nuclei were large, of rather uniform size characterizing the instantaneous nucleation and randomly distributed on the GC surface with a nuclei population density of ca. $2 \cdot 10^7$ cm^{-2} (Fig. 9a). From the comparison of the calculated (chronoamperometric) (Table 1) and measured (counting by AFM) values of N, the difference between them equal to about one order of magnitude was obtained. Such a phenomenon was already reported earlier [5, 6, 18]. The possible explanation for the difference was presented in the literature [5, 6]. It should be noted that the morphological picture observed here is relatively similar to that presented earlier [5, 6] for the comparable experimental conditions.

As is clear from the AFM in Fig. 9b, in the solution containing H_2SeO_3, the number of particles formed onto the electrode surface increases significantly; N was found to be equal to ca. $46 \cdot 10^7$ cm^{-2}, i.e. the difference between the values of N calculated from the chronoamperometric data (Table 1) and measured by the AFM technique holds almost unchanged. Although the estimation of N by a visual counting using the AFM images somewhat suffers from uncertainties depending on samples handling or a sensitivity of the method, it seems that, in the case under study, analogously as with a polycrystalline Pt electrode [18], such a method for the evaluation of N may be considered as being more reasonable.

Figure 10 shows the cross-sectional profiles of the surface along the lines as shown in the top view images. Form these profiles a lateral distance and height can be determined. It was found that, in the case of the pure acidic $CuSO_4$ solution (Fig. 10a), the ratio between the growth in the lateral direction and that in the vertical direction (x/z) was about 7.1, i.e. the growth in the x–y direction was more distinct. It was also obtained from the standard roughness measurements that the arithmetic roughness average, R_a, was 8.41 nm and the maximum height of the profile above a mean line, R_p, was ca. 97.8 nm. In the solution containing H_2SeO_3, the above mentioned ratio x/z was about 13.2, i.e. the lateral growth further becomes to be favoured. The parameters R_a and R_p were found to be ca. 8.4 nm and 34.2 nm, respectively, suggesting a smoothening effect under the influence of H_2SeO_3. Such an effect may be due to the formation of a certain surface compound at potentials more positive than E_{eq} for a couple Cu^{2+}/Cu^0. In the presence of this compound, somewhat analogously with oxygen-containing substances [32, 39], the Cu nucleation process seems to be strongly favoured.

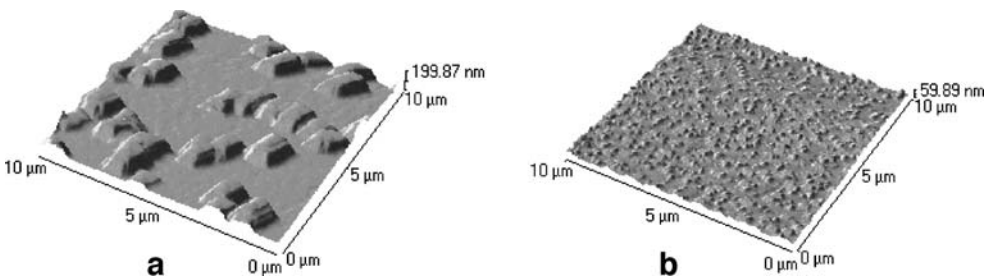

Fig. 9 Ex situ AFM images of GC electrode after Cu electrodeposition by E step from E_{start}= +0.80 V to E_{dep}=0.00 V for t_{dep} =5 s from 0.5 M H_2SO_4+0.01 M $CuSO_4$ solution without (**a**) or with 0.005 mM H_2SeO_3 (**b**)

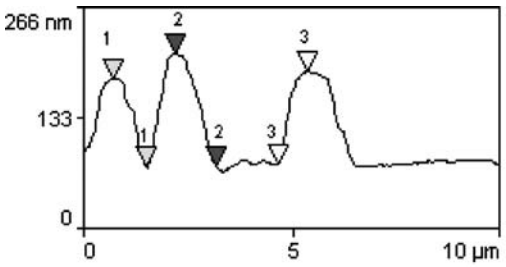

	Distance	Height
1	0.773 µm	104.8 nm
2	1.01 µm	136.7 nm
3	0.696 µm	110.8 nm

Standard Roughness	
Ra:	40.42 nm
Rp:	97.79 nm
Rpm:	50.64 nm
Rt:	143.3 nm
Rtm:	90.26 nm

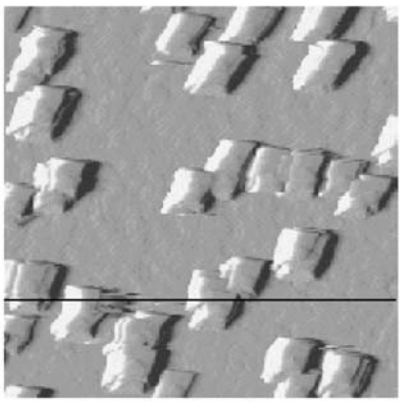

a

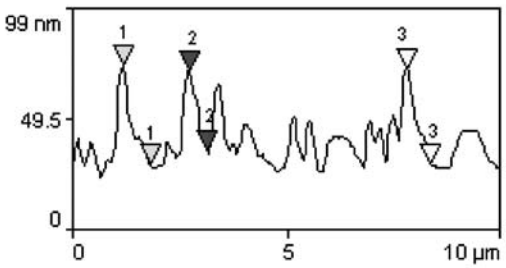

	Distance	Height
1	0.635 µm	44.48 nm
2	0.431 µm	35.28 nm
3	0.558 µm	42.40 nm

Standard Roughness	
Ra:	8.41 nm
Rp:	34.20 nm
Rpm:	23.46 nm
Rt:	50.35 nm
Rtm:	36.63 nm

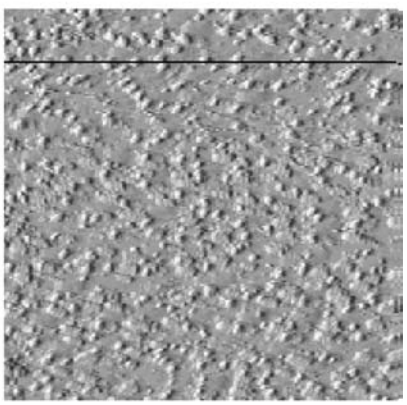

b

Fig. 10 Cross-sectional profiles along a selected line (from Fig. 9)

Undoubtedly, there can be several hypotheses relating the mechanism of the impact of H_2SeO_3 on the first stages of Cu electrocrystallization onto the GC electrode. Among them, the following one is suggested to be plausible. This suggestion is based on the simultaneous occurrence of two processes during the deposition of Cu from an acidic solution in the presence of the additive H_2SeO_3 namely, two one-electron transfer reactions [40–42] and a CORC [25–27].

It has been found for copper deposition/dissolution processes in acidic sulphate solutions that two consecutive one-electron transfer steps should be taken into account [40–42]. Then, following the considerations in the literature (e.g. [43]), the primary reaction scheme can be

$$Cu^{2+} + e \rightarrow Cu^{+} \quad (10a)$$

$$Cu^{+} + e \rightarrow Cu \quad (10b)$$

The redox process between Cu^{2+} and Cu^{+} has been supposed [40] to be the rate-limiting step (rds). A rate constant of the reaction (10a) has been found to be about three orders less then that for the reaction (10b) [44].

As far as the electrocrystallization of Cu in an acidic medium under the influence of the small amounts of H_2SeO_3 is concerned, the accelerating action of this additive on the Cu^{2+} discharge has been assumed to occur according to such CORC model [25, 26]:

$$H_2SeO_3 \rightarrow Se(0) \text{or} Se(-II) \quad (11a)$$

$$Se(0) \text{ or } Se(-II) + Cu^{2+} \rightarrow Se(IV) + Cu^{+}, \quad (11b)$$

i.e. the accelerating additive H_2SeO_3 provides a fast alternative chemical route to Cu^{+}. As this takes place, no evidence has been found for significant consumption of Se (IV), and it has been shown that its accelerating effect remains constant for a long period [25]. Besides, if the reduction of the additive at the electrode and its reoxidation by Cu^{2+}, reactions (11a) and (11b), respectively, are both fast compared with the reaction (10a), the CORC might be expected to become the main source of Cu^{+} [25].

Then, following the considerations presented earlier (see, e.g. [5] and partly [6, 7]), we assume that an additional amount of Cu^{+} at the surface of the working GC electrode obtained due to the CORC will result in the higher Cu nuclei population density N.

Conclusions

The analysis of the electrochemical data obtained with the GC electrode in the acidic $CuSO_4$ solution without or with H_2SeO_3 solution points to the instantaneous 3D nucleation and diffusion-controlled growth of Cu nuclei in accordance to the model proposed by Scharifker and Hills for the early stages of metal electrocrystallization onto a foreign substrate. The numerical values of electrocrystallization parameter such as a number of Cu nuclei N and an average nucleus radius r_{av} were evaluated from the chronoamperometric and AFM measurements following the usually used SH procedure. These parameters were shown to be dependent on the concentration of H_2SeO_3 and the deposition potential E_{dep}. The character of the dependences of N and r_{av} on the concentration of additive used in our study depends not only on the value of E_{dep}, but specifically on the region of Cu overpotentials. In particular, whereas in the region of lesser values of Cu overpotential these dependences are rather poorly described and less informative, at higher overpotentials they become well defined—N increases and r_{av} decreases with increasing the concentration of H_2SeO_3. The AFM measurements confirmed the smoothening effect of H_2SeO_3 during the electrodeposition of Cu onto the GC electrode from the acidic $CuSO_4$ solution. Some reasons causing the effect of smoothening under the influence of H_2SeO_3 were discussed. A possible explanation of the mechanism of the influence of H_2SeO_3 on the very beginning of the formation of the new Cu phase on the GC electrode was proposed.

References

1. Budevski E, Staikov G, Lorenz WJ (1996) Electrochemical phase formation and growth. VCH, Weinheim, New York, Basel, Cambridge, Tokyo
2. Martins ME, Salvarezza RC, Arvia AJ (1992) Electrochim Acta 37:2203
3. Margheritis D, Salvarezza RC, Giordano MC, Arvia AJ (1987) J Electroanal Chem 229:327
4. Štulíková M, Vydra F (1973) J Electroanal Chem 229:327
5. Grujicic D, Pesic B (2002) Electrochim Acta 47:2901
6. Danilov AI, Molodkina EB, Polukarov YM (2002) Rus J Electrochem 38:732
7. Danilov AI, Molodkina EB, Baitov AA, Pobelov IV, Polukarov YM (2002) Rus J Electrochem 38:743
8. Arzhanova T, Golikov A (2003) J Electroanal Chem 558:109
9. Milchev A, Zapryanova T (2006) Electrochim Acta 51:2926
10. Milchev A, Zapryanova T (2006) Electrochim Acta 51:4921
11. Zapryanova T, Hrussanova A, Milchev A (2007) J Electroanal Chem 600:311
12. Gunawardena GA, Hills GJ, Montenegro I (1978) Electrochim Acta 23:693
13. Gunawardena GA, Hills G, Montenegro I, Scharifker B (1982) J Electroanal Chem 138:225
14. Scharifker B, Hills G (1983) Electrochim Acta 28:879
15. Scharifker BR, Mostany J (1984) J Electroanal Chem 177:13
16. Heerman L, Tarallo A (1999) J Electroanal Chem 470:70
17. Šimkūnaitė D, Steponavičius A, Jasulaitienė V, Matulionis E (2003) Trans Inst Metal Finish 81:199
18. Šimkūnaitė D, Ivaškevič E, Kaliničenko A, Steponavičius A (2006) J Solid State Electrochem 10:447

19. Mishra KK, Rajeshwar K (1989) J Electroanal Chem 271:279
20. Carbonelle P, Lamberts L (1992) Electrochim Acta 37:1321
21. Massaccesi S, Sanchez S, Vedel J (1993) J Electrochem Soc 140:2540
22. Gomez H, Schrebler R, Cordova R, Ugarte R, Dalchielle EA (1995) Electrochim Acta 40:267
23. Lippkow D, Strehblow H-H (1998) Electrochim Acta 43:2131
24. Marlot A, Vedel J (1999) J Electrochem Soc 146:177
25. Hill MRH, Rogers GT (1976) J Electroanal Chem 68:149
26. Lezhava TI (1989) Acceleration at metal deposition. Diss. Frumkin Inst Electrochem, Moscow
27. Steponavičius A, Šimkūnaitė D, Jasulaitienė V (1997) Chemija No 2:64
28. Zuman P, Somer G (2000) Talanta 51:645
29. Jarzabek G, Kublik Z (1980) J Electroanal Chem 114:165
30. Skyllas Kazacos M, Miller B (1980) J Electrochem Soc 127:869
31. Espinosa AM, Tascón ML, Vázquez MD, Batanero PS (1992) Electrochim Acta 37:1165
32. Danilov AI, Molodkina EB, Polukarov YM (2000) Rus J Electrochem 36:987
33. Hyde ME, Compton RG (2003) J Electroanal Chem 549:1
34. Milchev A, Heerman L (2003) Electrochim Acta 48:2903
35. Mirkin MV, Nilov AP (1990) J Electroanal Chem 283:35
36. Brylev O, Roué L, Bélanger D (2005) J Electroanal Chem 581:22
37. Quickenden TI, Xu Q (1996) J Electochem Soc 143:1248
38. Leone A, Marino W, Scharifker BR (1992) J Electrochem Soc 139:438
39. Danilov AI, Molodkina EB, Polukarov YM (2000) Rus J Electrochem 36:998
40. Mattsson E, Bockris JO'M (1959) Trans Faraday Soc 55:1586
41. Bockris JO'M, Enyo M (1962) Trans Faraday Soc 58:1187
42. Brown OR, Thirsk HR (1965) Electrochim Acta 10:383
43. Burrows IR, Harrison JA, Thompson J (1975) J Electroanal Chem 58:241
44. Albaya HC, Lorenz WJ (1972) Z Phys Chem NF 81:294